

New Phytologist Supporting Information

Article title: NIN is essential for development of symbiosomes, suppression of defence and premature senescence in *Medicago truncatula* nodules

Authors: Jieyu Liu, Menno Rasing, Tian Zeng, Joël Klein, Olga Kulikova, and Ton Bisseling

Article acceptance date: 30 November 2020

The following Supporting Information is available for this article:

Fig. S1 Expression profile of *Medicago* NIN/Medtr5g099060 (probe id. Mtr.28094.1.S1.st) based on *M. truncatula* Gene Atlas in various tissues.

Fig. S2 Live/dead staining shows prematurely death of rhizobia in *Medicago nin-16* nodules.

Fig. S3 *Medicago nin-13* mutant nodules show the same phenotype as *nin-16*.

Fig. S4 F1 plants obtained by crossing *Medicago nin-13* and *nin-16* showed the same nodule phenotype as the parental plants.

Fig. S5 *NF-YA1* expression pattern in *Medicago nin-16* nodule.

Fig. S6 *Tnt1* was transcribed in *Medicago nin-13* and *nin-16* mutant nodules.

Fig. S7 *NIN* RNA transcribed from the *Medicago nin-16* allele was altered by *Tnt1* insertion.

Fig. S8 Complementation of *Medicago nin-16* nodule phenotype with *ProNIN_{3C-5kb}:NIN Δ PB1* and *ProNIN_{3C-5kb}:NIN*.

Table S1 Primers used in this study.

Table S2 Genes with transcripts detected in *Medicago nin-16* or R108 (wild type). (separate Excel file)

Table S3 Genes differentially expressed in *Medicago nin-16*. (separate Excel file)

Table S4 Genes specifically expressed in different *Medicago* wild type nodule developmental

zones differentially expressed in *nin-16*. (separate Excel file)

Table S5 Differentially expressed gene families/metabolism pathways in *Medicago nin-16*

(separate Excel file)

Fig. S1 Expression profile of *Medicago NIN*/Medtr5g099060 (probe id. Mtr.28094.1.S1.st) based on *M. truncatula* Gene Atlas in various tissues. Mt *NIN* is specifically expressed in nodules.

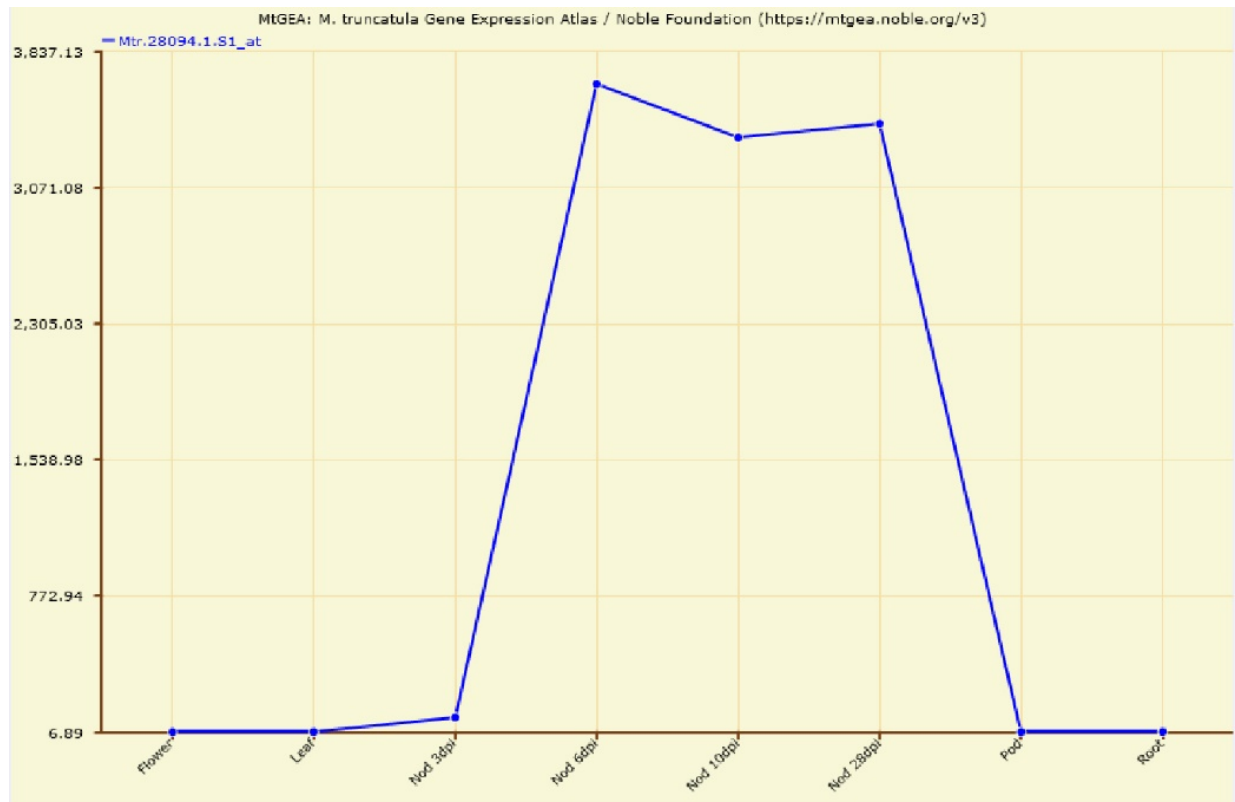


Fig. S2 Live/dead staining shows prematurely death of rhizobia in *Medicago nin-16* nodules. Sections of two weeks post inoculation (wpi) nodules, imaged by a confocal microscope after live/dead staining assay. Green (SYTO 9) and red (propidium iodide) stain alive and dead bacteria respectively. Compare with wildtype (a, b), the early death of the bacteria in the *nin-16* nodule was detected (c, d). Bars: (a, c) 250 μm and (b, d) 50 μm .

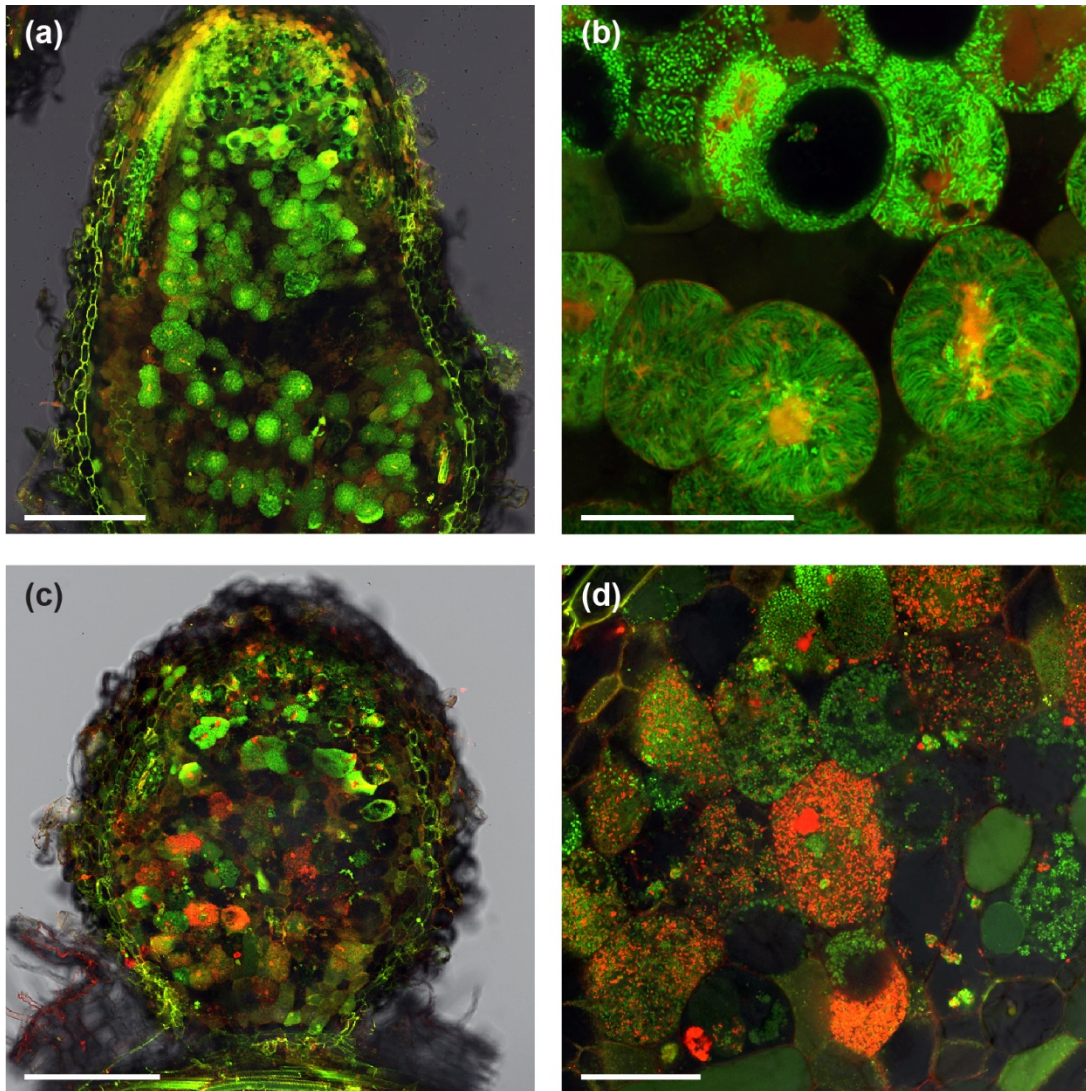


Fig. S3 *Medicago nin-13* mutant nodules show the same phenotype as *nin-16*. Like *nin-16*, *nin-13* formed white nodules at two wpi (a). Inoculation with rhizobial carrying *nifH::GFP* showed that *nifH* was not induced in *nin-13* nodules (e). Sections of these nodules showed that meristem was formed (b), rhizobia were released and divided (c), but bacteria differentiation were arrested, and premature senescence was induced (d). The bacteria death was confirmed by live/dead staining (f, g). Green (SYTO 9) and red (propidium iodide) stain alive and dead bacteria respectively. Potassium permanganate/methylene blue staining shows accumulation of phenolic compound in *nin-13* nodules (h). Bars: (a) 2 mm; (b) 300 μ m; (c, d, g) 30 μ m; (e, f) 250 μ m and (h) 500 μ m.

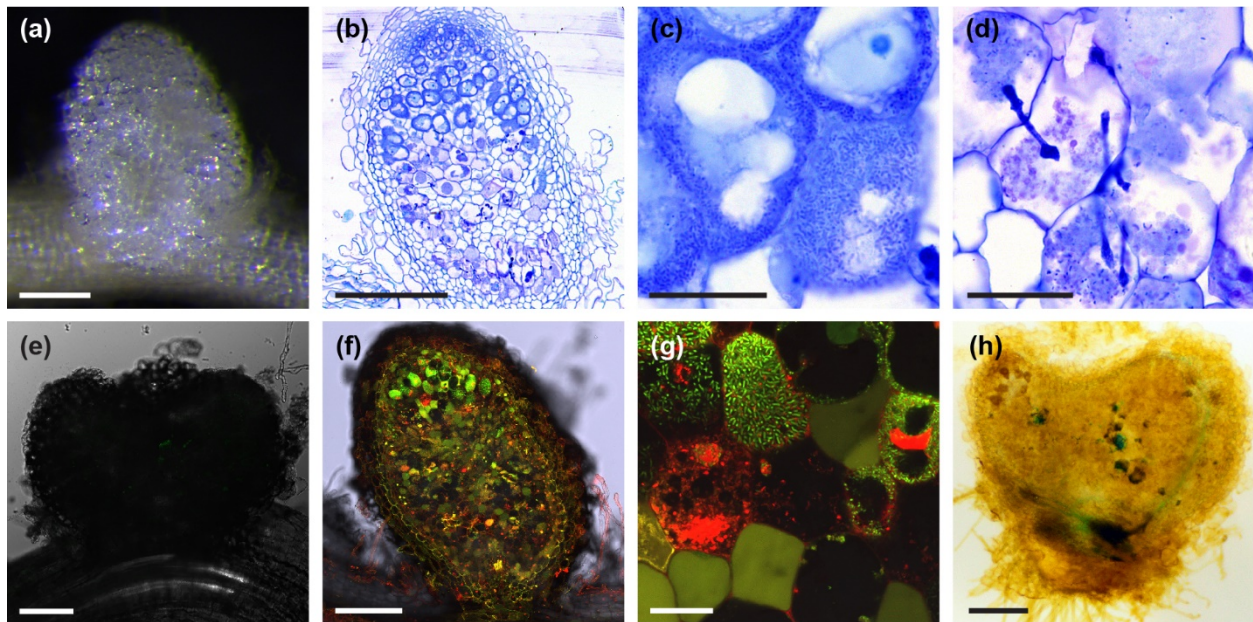


Fig. S4 F1 plants obtained by crossing *Medicago nin-13* and *nin-16* showed the same nodule phenotype as the parental plants. Transmitted light macroscopy images of root nodules formed F1 plants obtained by crossing *nin-13* and *nin-16* (a). Semi-thin sections of these nodules stained with toluidine blue display the same nodule phenotype as the *nin-13* and *nin-16* (b). Bars: (a) 2 mm and (b) 300 μ m.

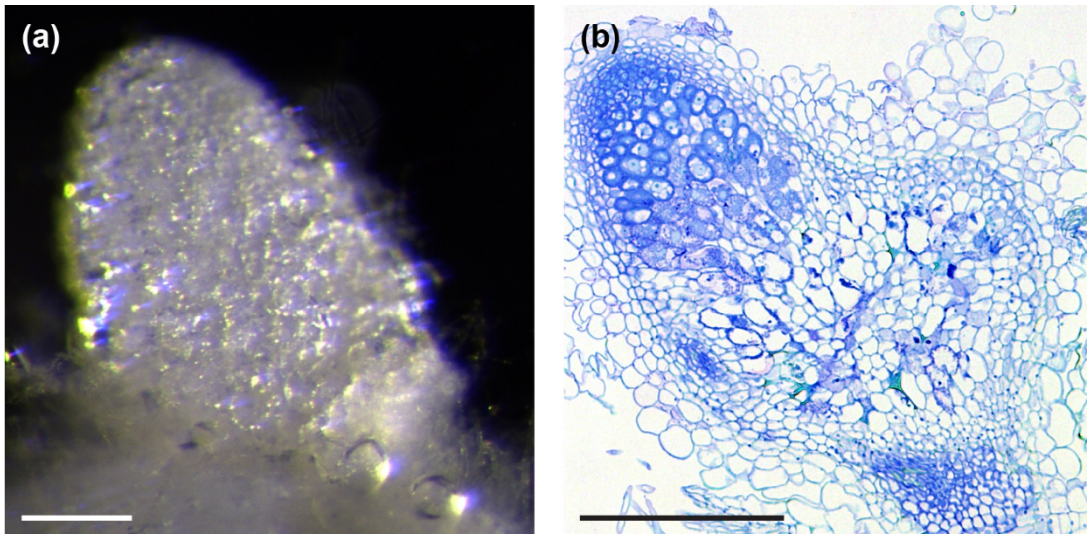


Fig. S5 *NF-YA1* expression pattern in *Medicago nin-16* nodule. RNA *in situ* localization of *NF-YA1* in *nin-16* nodule at two wpi. Hybridization signals are visible as red dots. Scale bar: 200 μ m.

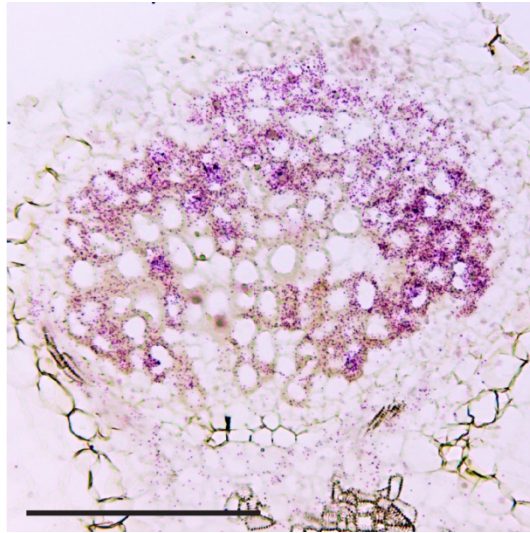


Fig. S6 *Tnt1* was transcribed in Medicago *nin-13* and *nin-16* mutant nodules. Quantitative real-time (qRT-PCR) using different primer sets targeting *NIN*, upstream junction of *NIN* and *Tnt1* (*NIN-Tnt1*), within *Tnt1* insertion (*Tnt1*) and downstream junction of *Tnt1* and *NIN* (*Tnt1-NIN*) show that *Tnt1* was transcribed in *nin-13* (a) and *nin-16* (b) nodules. Data are means \pm SD of three biological replicates.

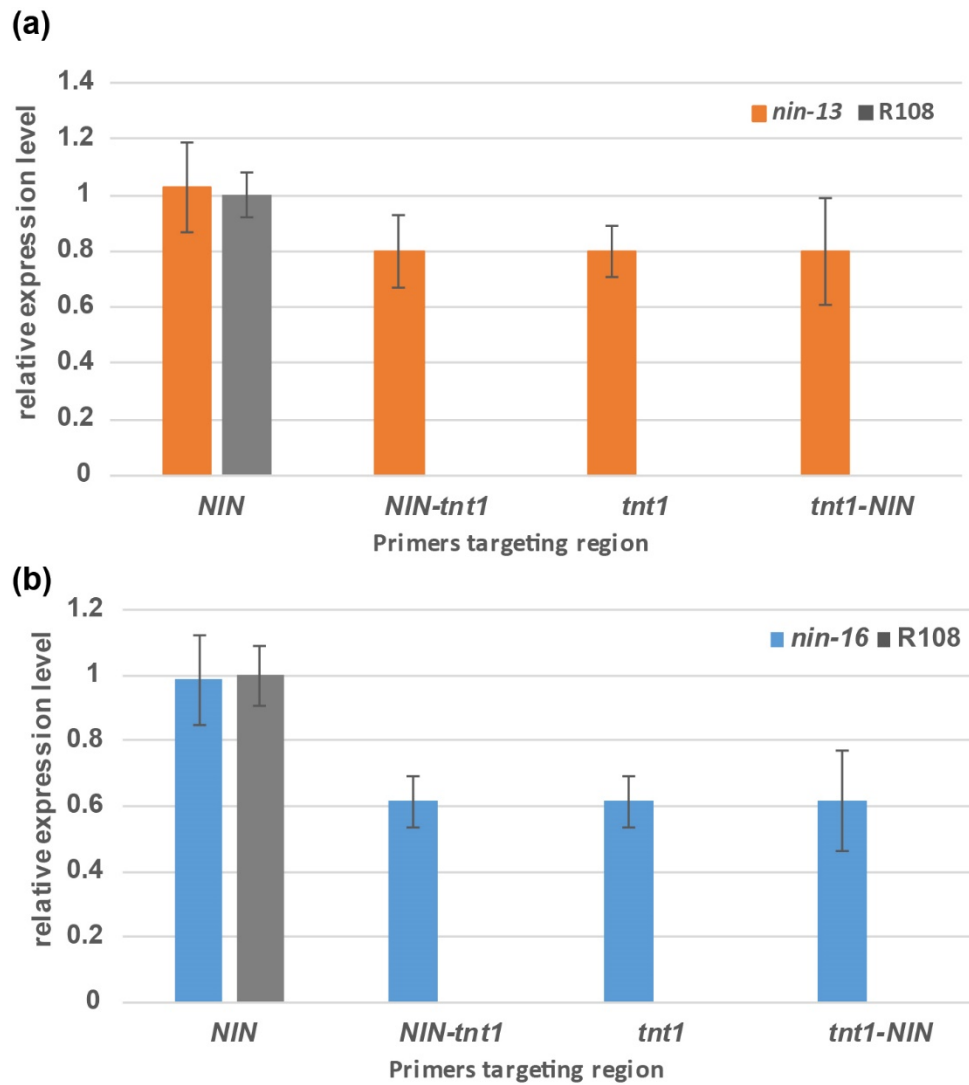
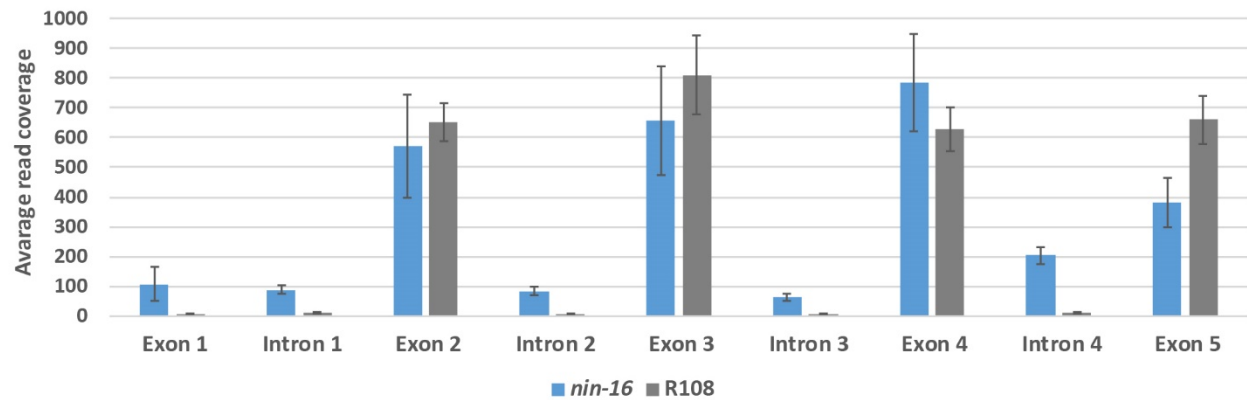


Fig. S7 *NIN* RNA transcribed from the Medicago *nin-16* allele was altered by *Tnt1* insertion. (a) Mapping of the reads at the *NIN* locus in R108 (above) and *nin-16* (below). Arrow heads indicate the reads that mapped in *NIN* intron regions and arrow indicates the much longer 5' UTR in *nin-16*. (b) Quantification of average read coverage for each exon/intron region of *NIN* in *nin-16* and R108. The read coverage was determined with mosdepht (version 0.3.0) using default settings (Pedersen & Quinlan, 2018). Data are means \pm SD. (c) Non-spliced intron rate of *NIN* RNA in *nin-16* and R108. Non-spliced intron rate was calculated by intron reads coverage divided by the average exon reads coverage. Calculation of average read coverage in exon regions were based on the exons 2, 3 and 4. This is because *nin-16* contains a *Tnt1* insertion in exon 5 which leads to low read coverage, and exon 1 is in the non-coding region and there the read coverage is much lower than in the coding region. The average read coverage in exons of R108 and *nin-16* were similar, in R108 it is 697.23 and in *nin-16* it is 671.39. Theoretically it is possible that only one or all introns are aberrantly spliced. Therefore, we can only indicate a range within which the transcripts are wrongly spliced. The frequency of aberrantly spliced *NIN* transcripts in *nin-16* is between 30.24% (all introns are aberrantly spliced) and 64.80% (a single intron is aberrantly spliced). This is markedly higher than the frequency in R108 which is between 1.39% and 4.37%.

(a)



(b)



(c)

Non-spliced intron rate of *NIN* in R108 and *nin-16*

	Intron 1	Intron 2	Intron 3	Intron 4	Sum intron 1-4
R108	1.39%	0.66%	0.95%	1.38%	4.37%
<i>nin-16</i>	12.98%	12.26%	9.32%	30.24%	64.80%

Fig. S8 Complementation of *Medicago nin-16* nodule phenotype with *ProNIN_{3C-5kb}:NIN Δ PB1* and *ProNIN_{3C-5kb}:NIN*. Overview (a, c, e) and close-up (b, d, f) images of semi-thin longitudinal sections of nodules formed on *nin-16* roots transformed with *ProNIN_{3C-5kb}:NIN Δ PB1* (a, b), *ProNIN_{3C-5kb}:NIN* (c, d) and empty vector (e, f). Fully elongated symbiosomes were observed in five out of 30 sectioned nodules formed on *nin-16* roots transformed with *ProNIN_{3C-5kb}:NIN Δ PB1* and five out of 60 nodules formed on *nin-16* roots transformed with *ProNIN_{3C-5kb}:NIN*, but not in nodules formed on the roots transformed with empty vector (n=55). In addition, the defence-related phenotype was markedly reduced in the complemented nodules. Bars: (a, c, e) 300 μ m and (b, d, f) 30 μ m.

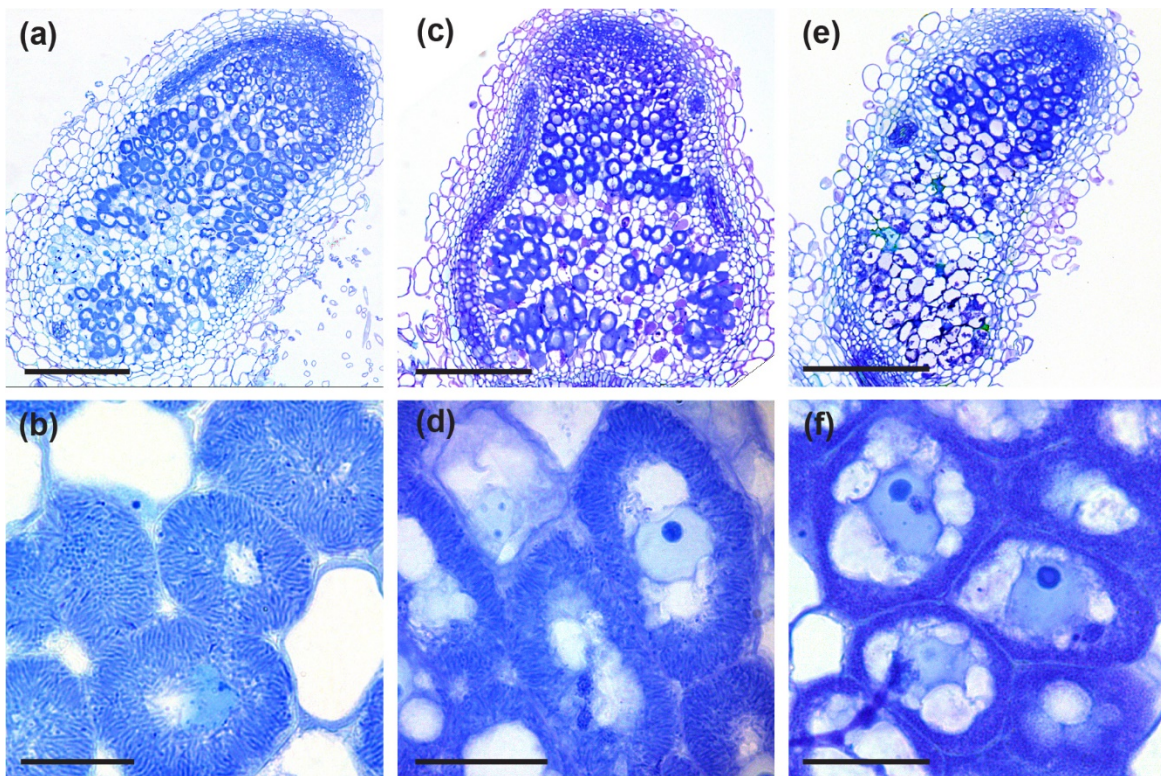


Table S1 Primers used in this study.

Name	Sequence (5'→3')
qPCR-NIN-F	TACTTTGCCGGAAGCCTAAA
qPCR-NIN-R	ATCTGTATGGCACCCCTCTGC
qPCR-NIN-Tnt1-F	GAGTTGATCATGCCTTCATGC
qPCR-NIN-Tnt1-R	GGTTGGCTACCAAACCAAAG
qPCR-Tnt1-F	GCGTTTAAAATCCCAGAGAG
qPCR-Tnt1-R	AACCGAACACCTTCAGATGC
qPCR-Tnt1-NIN-F	TCAGAAGGGTTTTCCACGTAA
qPCR-Tnt1-NIN-R	CCACAGTTGGTCTTGGAGGT
qPCR-ACTIN2-F	TGGCATCACTCAGTACCTTTCAACAG
qPCR-ACTIN2-R	ACCCAAAAGCATCAAATAATAAGTCAACC
Genotyping-NIN-F	TGCTAATGGTGGTGATGGTAAT
Genotyping-NIN-R	GGTTAAATCGCCTTGCAATCTC
Genotyping-Tnt1-R	TGTAGCACCGAGATACGGTAATTAACAAGA
NIN _{ΔPB1} -F	CACCATGGAATATGGTGGTGGGTT
NIN _{ΔPB1} -R	GTAGTCCTGGATATTAATATTAGATGCA
NIN _{ΔPB1} -35Ster-BP-F	GGGACAGCTTTCTTGTACAAAGTGAAATGGAATATGGTGGTGGGTTAGTG
NIN _{ΔPB1} -35Ster-BP-R	GGGACAACCTTTGTATAATAAAGTTGCTCACTGGATTTTGGTTTTAGGAATTA
NIN-CDs-F	CACCATGGAATATGGTGGTGGGTTAGTGG
NIN-CDs-R	GCTAGGAGGATGGACTGCTGCTGCT
NINGFP-35Ster-BP-F	GGGACAGCTTTCTTGTACAAAGTGAAATGGAATATGGTGGTGGGTTAGTG
NINGFP-35Ster-BP-R	GGGACAACCTTTGTATAATAAAGTTGCTCACTGGATTTTGGTTTTAGGAATTA
GFPNIN-35Ster-BP-F	GGGACAGCTTTCTTGTACAAAGTGAAATGGTGAGCAAGGGCGAGGA
GFPNIN-35Ster-BP-R	GGGACAACCTTTGTATAATAAAGTTGCTCACTGGATTTTGGTTTTAGGAATTA

Sequences designated in boldface are added to primers for TOPO cloning or BP recombination

References:

Pedersen BS, Quinlan AR. 2018. Mosdepth: Quick coverage calculation for genomes and exomes. *Bioinformatics* **34**: 867–868.